

Article

Impact of Landscape Factors on Automobile Road Deformation Patterns—A Case Study of the Almaty Mountain Road

Ainur Kairanbayeva ¹, Gulnara Nurpeissova ^{2,3,*} , Zhumabek Zhantayev ¹, Roman Shults ⁴, Dina Panyukova ², Saniya Kiyalbay ² and Kerey Panyukov ³

¹ Institute of Ionosphere, National Center of Space Research and Technology, Almaty 050020, Kazakhstan

² L.B. Goncharov Kazakh Auto Road Institute (KazADI), Almaty 050061, Kazakhstan

³ Engineering Institute, Caspian University, Almaty 050000, Kazakhstan

⁴ Department of Geomatics, Faculty of Civil Engineering, Czech Technical University in Prague, 166 29 Prague, Czech Republic

* Correspondence: kerey97@mail.ru

Abstract: The geography of Kazakhstan is characterized by a diverse landscape and a small population. Therefore, certain automobile roads pass through unpopulated mountain regions, where physical road diagnostics are rare or almost absent, while landscape factors continue to affect the road. However, modern geo-information approaches and remote sensing could effectively provide the road diagnostics necessary to make timely control decisions regarding a road's design, construction, and maintenance. To justify this assumption, we researched the deformation of a mountain road near Almaty city. Open access satellite images of and meteorological archival data for the region were processed. The resulting data were compared to validate the road's deformation triggers. Extreme weather conditions' impacts could be identified via road destruction (nearly 40 m longitudinal cracks, 15 m short transversal cracks, and two crack networks along a 50 m road section). The remotely sensed parameters (vertical displacement velocity, slope exposure, dissections, topographic wetness index, aspect, solar radiation, SAVI, and snow melting) show the complexity of triggers of extensive road deformations. The article focuses only on open access data from remote sensing images and meteorological archives. All the resulting data are available and open for all interested parties to use.

Keywords: road deformation; open data; remote sensing; meteorological data; data digitization; data analytics; impact assessment; multiple criteria evaluation; decision-making support



Citation: Kairanbayeva, A.; Nurpeissova, G.; Zhantayev, Z.; Shults, R.; Panyukova, D.; Kiyalbay, S.; Panyukov, K. Impact of Landscape Factors on Automobile Road Deformation Patterns—A Case Study of the Almaty Mountain Road. *Sustainability* **2022**, *14*, 15466. <https://doi.org/10.3390/su142215466>

Academic Editors: Elżbieta Macioszek, Margarida Coelho, Anna Granà and Raffaele Mauro

Received: 7 October 2022

Accepted: 17 November 2022

Published: 21 November 2022

Publisher's Note: MDPI stays neutral with regard to jurisdictional claims in published maps and institutional affiliations.



Copyright: © 2022 by the authors. Licensee MDPI, Basel, Switzerland. This article is an open access article distributed under the terms and conditions of the Creative Commons Attribution (CC BY) license (<https://creativecommons.org/licenses/by/4.0/>).

1. Introduction

Nowadays, in Kazakhstan, a huge amount of time, as well as human and financial resources, is spent designing and building international transit road infrastructure due to the “Western Europe–Western China” route following the historical “Silk Road” being built throughout the territory of the republic. This transport network historically brought economic, social, and cultural development to central Asia and positively affected international relationships and cooperation between all concerned parties. However, any road infrastructure requires both reasonable construction and timely maintenance. The development of maintenance techniques starts with analyses of and field research on road pavement [1]. The main part of the Kazakhstan transport network passes through underpopulated territories, which leads to complications when attempting to monitor roadbeds. When considering the geographical features involved, the classical “field” monitoring of automobile roads' states would lead to huge financial expenses, and the use of remote sensing could simplify the task tremendously. Additionally, a number of automobile roads in the republic pass through mountain regions and are exposed to geological processes. For example, several mountainous automobile roads that are near the biggest city in Kazakhstan—Almaty—are routinely damaged by landscape and weather changes. Therefore, the timely control of the design, construction, and maintenance of mountain automobile roads requires the

implementation of modern geographic information systems that consider the landscape dynamics near automobile roads. Moreover, the entities that manage local roads lack the human, financial, informational, and technological resources to provide regular state-of-the-art road diagnostics in a timely manner. This has resulted in a local demand for a remote road diagnostic and forecasting methodology based on open access sources.

One of the techniques for predicting the operating roadbed's state requires data about the material of the roadbed and its base (which is usually absent from open source data), meteorological data, data about the road's load, and other operative data [2]. Road authority departments usually collect roads' load data. Meteorological data are collected by countries' meteorological stations. It is recommended that a roadbed's actual parameters be estimated by non-destructive control methods, e.g., the measurement of the longitudinal and transversal unevenness of a road, the orientation and rise of a roadbed, the longitudinal and transversal slopes, video diagnostics, the measurement of friction and longitudinal displacement, and geo-radar scanning. One of the most important parameters in the diagnosis of a roadbed's state is the identification of cracks in a roadbed [3]. This is very complex process when conducted in the field, and it includes tasks such as crack search, analysis, classification, and depth measurement. It is suggested that detailed identification be conducted via optical methods (a LIDAR and video fixation with following assessments via mathematical and intellectual methods). Moreover, it is strongly recommended that parameters such as the evenness of a roadbed be considered [4]. The materials' features can be examined via two main approaches: the long-term monitoring of a roadbed in a laboratory with a special road load simulator or field research on a roadbed using a mobile durometer [5]. A complex approach involving building information modeling (BIM) tools has also been suggested [6]. An Internet-of-Things approach was suggested that used sensors in the pavement which indicated its state in real time [7]. Low-cost methodologies and indicators installed on smartphones are applied for road diagnostics in developing countries [8]. Most of these approaches cannot be implemented in the republic of Kazakhstan, as there is lack of both financial and human resources for detailed field diagnostics of huge lengths of road.

The authors looked at scientific research conducted in Europe, America, and Asia on landscape factors affecting the sustainable development of territories, particularly transport infrastructure. One of the research studies showed that the classical mathematical models of landscape movements are formulated on the basis of nonobjective data, as each model considers only some of the key factors [9]. However, if the factors that are not considered play a significant role, the model's predictions will not reflect reality [10]. Academics have reached a consensus that the best method is the parallel usage of different approaches and models, along with the regular tracking of critical parameters by remote sensing [11]. A remote sensing method has been used in research on precipitation data to construct an early warning system for deadly landslides in Indonesia [12]. Chinese authors have suggested combining remote images with synthetic-aperture radar (SAR) images and optical measurements to track the historical changes in rock formations in the context of landscape movement [13]. The scientific literature substantiates the use of synthetic-aperture radar (SAR) images for the remote sensing of landscape changes under all climatic and geographic conditions [14]. Remote sensing technologies have also been applied to indicate landscape dynamics in Russia and Kyrgyzstan [15,16].

Severe landscape movements' impacts on automobile roads' states and, by extension, the whole transport network have been studied in Austria, on Oahu Island in the Hawaiian archipelago, in Reggio Calabria, Italy, in Taiwan, and in Mexico [17–21]. Italian researchers have also used data from different sources, including remote sensing, for the forecasting of a roadbed's wearing out as a result of landscape changes. The estimation of roads' states has also been conducted using Google Street View images [22]. The authors of this study suggest the use of remotely sensed parameters to detect even slight landscape dynamics in order to compare these results with the road state, as assessed by a field road laboratory.

The exact abovementioned methodologies cannot be applied directly in our case due to the narrow focus and local specifics, but they can be combined under the assumption that timely automobile road diagnostics are possible to acquire from open data sources from remote sensing and meteorological archives. To verify this assumption, the authors also assessed the automobile road's operational characteristics by means of a road laboratory. Afterwards, we compared the field data with the data from meteorological archives and remote sensing data from cosmic images near the automobile road collected by WorldView-1, 2, 3, GeoEye-1, Sentinel-1-2, and other satellites. The comparative analysis shows that the roadbed's state correlates well with the remotely sensed landscape parameters and the meteorological conditions. All considered data are available and open for all interested parties to use.

2. Study Area

2.1. General Geographical Characteristics of the Region

Kazakhstan is located in the center of Eurasia and covers a territory of 2,724,900 square kilometers [23]. Most of its territory is in Asia, but a small part is in Europe. In the north and west, the republic borders Russia (the border is 7591 km long and is the longest continuous land border in the world), in the east it borders China (1783 km-long border), and in the south it borders Kyrgyzstan (1242 km-long border), Uzbekistan (2351 km-long border), and Turkmenistan (426 km-long border). The land borders' total length is 13,392.6 km. The length of the country from east to west is 2963 km, and from north to south, it is 1652 km. The country also borders the inland Caspian and Aral Seas. Kazakhstan has no access to the sea and is the world's largest landlocked country.

The territory of Kazakhstan occupies the southeastern part of the East European craton (Caspian sedimentary basin) and the western, southwestern, and southern parts of the Central Asian Orogenic Belt, in the southwest of which there is a vast flat area, the Turan plate, that is covered by a Meso-Cenozoic cover, under which are the linear paleozooids of the Mugodzhary and Karatau mountains [24]. To the east of the Turan plate, the Central Kazakhstan Paleozoic massif stands out, as well as the Saryarka, Chingiz-Tarbagatai, and Zaisan linear folded systems, part of the Altai-Sayan folded region, the sub-latitudinal alpine belt of the Northern Tien Shan, and the Dzungarian Alatau.

The relief of Kazakhstan is extremely diverse, but most of the territory consists of plains, low mountains, and hills. In the central region of the country lie the Kazakh uplands ("Sary-Arka" (Yellow steppe) in Kazakh), which are west of the Turgai plateau. The entire northern part of the country is located on the West Siberian Plain. Just south of the plain lie the small mountains of Kokshetau (Blue Mountains). The western part of the country is located for the most part on the East European Plain, on which the Caspian Lowland and the Sub-Ural Plateau are located. In the west of Kazakhstan, there are the low Mugodzhary Mountains—the southern extension of the Ural Mountains. On the Mangyshlak peninsula, the Karagie (Batyra) depression is 132 m below sea level. To the east of the Mangyshlak peninsula, the Ustyurt plateau extends, the edges of which form high ledges (chinks). In the east of Kazakhstan, the Altai and Tarbagatai mountains rise, separated by Lake Zaisan. The ridges of the northern outskirts of Tien Shan stretch from the southern to the eastern part of Kazakhstan along the borders with Kyrgyzstan and China. They reach almost seven thousand meters above sea level at the junction of the borders of Kazakhstan, Kyrgyzstan, and China (Khan-Tengri peak, 6995 m). In the southeast of the country lie the Dzungarian Alatau and Zailiysky Alatau ridges, and at the foot of the Zailiysky Alatau is the former capital of Kazakhstan and the largest city in the country—Almaty.

Kazakhstan has a sharp continental climate with hot summers and very cold winters. The capital of Kazakhstan is the second coldest capital in the world after Ulaanbaatar. Fallouts vary between arid and semi-arid conditions, with winters being particularly dry. The atmospheric circulation over Kazakhstan is strongly influenced by the republic's surface characteristics. Mountain ranges in the southern, southeastern, and eastern parts of the republic are natural barriers for the passage of cold air masses to the south.

Kazakhstan mainly comprises plain low-mountain regions with wide, flat lowlands and depressions, sometimes even below sea level. The surface consists of tablelands and low-mountain masses. There are snow-capped high-mountain regions along the eastern and southeastern borders of the republic.

Kazakhstan has four climatic zones: forest steppe, steppe, semi-desert, and desert [25]. Their characteristics are presented in Table 1.

Table 1. Characteristics of climatic zones in Kazakhstan [25].

Climatic Zone	Fallouts		January		July		Details
	Annual Number, mm	In Warm Period, %	Annual Temp., °C	Extreme Values, °C	Annual Temp., °C	Extreme Values, °C	
Forest steppe	320–360	80	−17	−(42–48)	20	41	Winter is long and cold, late spring and early fall have windchills, winter temperature rises up to +5 °C.
Steppe	230–340	65–80	−(15–19)	−(42–54)	19–23	40–42	Percent of winter fallouts up to 23–27% of the annual value, potential strong winds and snow windrows, 20–80 days of dust storms, long and hot summer.
Semi-desert	134–330	55–70	−(10–20)	−(37–50)	21–25	40–45	High frequency of atmospheric drought and drought wind weather.
Desert	100–200	46–60	−(5–15)	-	-	-	The soil surface can heat up to 70 °C in the daytime and cool to 0 °C at night.

Table 1 shows that the temperature range for every climatic zone within the republic is enormous. It can differ from +40 °C in summertime to −40 °C in winter. The situation is similar when it comes to fallouts. While the annual average is rather low, the rare fallouts are heavy. These variations put additional restrictions on any introduced construction.

The population, according to the estimate of the State Statistics Committee as of 1 July 2022, is 19,246,300 people [26]. The population density is among the lowest in the world at less than seven people per square kilometer.

Kazakhstan is implementing a large-scale project named “The New Silk Road”, which should revive the country’s historical role as the main connecting link of Eurasia and turn it into the largest business and transit hub in the region—a kind of bridge between Europe and Asia [27]. At present, the total length of the road network in the Republic of Kazakhstan is 96,000 km, including 25,000 km of republican roads, 89% of which are in normal condition, and 71,000 km of local roads, 75% of which are in normal condition.

The maintenance and restoration of roads of such length require many financial and human resources. A group of scientists proposed a methodology for analyzing the collective road surface data to implement a network-level road management program in Kazakhstan. That methodology is based on a study of roads in the Kostanai region [28]. The study was based on a dedicated road asset management system (RAMS) developed in 2017, which was supposed to serve about 23,500 km of roads that make up the main road network of Kazakhstan (republican roads) and also includes six international corridors. In the first attempt to create a digital database and to engage in network maintenance management for budget optimization through an economic analysis, an obligatory component, beside the data on traffic’s influence on pavements, is the collection and processing of data about the pavement’s surface damage [29]. The data are collected via continuous digital image fixation and automated methods for detecting cracks as the type of damage to the pavement surface made by traffic moving in forward and reverse directions. However, in recent years, new roads have been actively built and work has been regularly carried out to repair and restore them, so the data from this database are outdated. Moreover, the proposed methods do not take into account the impact of geological and climatic factors on the state of the road surface, and most of the used data are from closed databases. Therefore, it remains necessary to provide timely automobile road diagnostics based on open data from remote sensing and meteorological archives in the region.

2.2. Characteristics of the Research Area

The verification of our assumption requires field data regarding mountain roads within the republic. Due to the limitation of the project budget, the road should be easily accessible for the road laboratory and research group, so the Almaty Region was considered (see the center of Figure 1). At the same time, the road should be lightly used to imitate an underpopulated region. The Almaty–Cosmostation road, shown on the left of Figure 1, matches these requirements. It is a mountain automobile road with a complex landscape. It is accessible from the scientific capital of the republic—Almaty city. The road is open only for Cosmostation access and state transport due to ecological restrictions, meaning that it has a low traffic load.

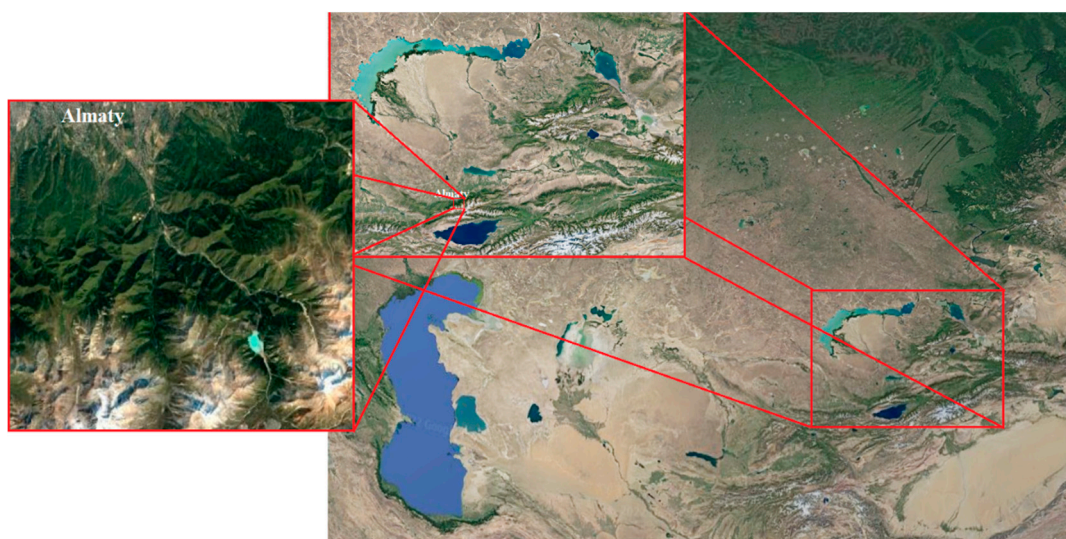


Figure 1. Research area within the Republic of Kazakhstan.

The Almaty–Cosmostation road passes through gorges in the Trans-Ili Alatau, North Tian Shan. The highest part of the road is 3336 m above sea level. The road’s length from Al-Farabi Street in Almaty up to the Cosmostation is nearly 34 km.

3. Methodology

This research considers data from three specific scientific areas: road engineering, meteorology, and remote sensing. All three apply different methods to collect and assess data. The main goal of the research is to compare all three datasets. Therefore, the methodology contains three main parts: the road diagnostic methodology, the meteorological impact, and the choice of remotely sensed parameters.

3.1. Road Diagnostic Methodology

Road diagnostics in Kazakhstan are provided according to state standards [30,31].

Managing decisions regarding roads within the republic are made based on road diagnostics formalized by a score from regulatory documentation, where the road’s state can be divided into three categories, with the following features:

1. The roadbed is solid, the transversal profile is preserved, road cover deformation and defects are absent, and single cracks at intervals of more than 40 m are permissible;
2. Between 5% and 30% deformed cover (specified for each cover type) showing inadequate strength of the roadbed, single transversal profile distortion;
3. Clear deformations several-fold more severe showing the inadequate strength of the roadbed, unstable holes in crack networks, and occasional ruptures.

Group I is additionally divided into four subgroups:

1. Smooth cover, no deformations;

2. Smooth cover with occasional rare deformations not affecting traffic conditions, velocity, or safety;
3. The road has small unevenness, widely spaced cracks, and an insignificant number of other deformations;
4. The road has significant unevenness, corrugations, raveling, and other deformations affecting traffic conditions and velocity. In addition, edge failures in the road cover are possible [30].

More detailed diagnostics according to state regulatory documentation should be provided by field measurements of short critical sections within the road [31]. They consist of field measurements of each critical sections, such as:

- Visual assessment of the road pavement and road bed;
- Measurement of the road's transversal and longitudinal unevenness at three points (beginning, middle, and end) using a 3 m-long staff;
- Measurement of the road bed depth;
- Measurement of the pavement's transversal and longitudinal friction coefficient using a portable IKSp device;
- Measurement of the road pavement's hardness using a BeldorNII durometer;
- Assessment of the pavement's width using a sliding caliper;
- Assessment of the transversal, longitudinal, and diagonal crack lengths using a measuring tape and curvimeter.

As the road pavement is one year old, most of the parameters are in a normal state. Its unevenness and hardness are affected by the lack of use of high-profile pneumatic and vibrating rollers. The main differences between the chosen sections are the transversal, longitudinal, and diagonal cracks' lengths and specific deformations, which will be compared in Section 4.1.

There is more information about the measuring instruments, techniques, and registered road characteristics in the authors' previous article [9].

3.2. Meteorological Impact

This project aims to identify factors affecting the roadbed. Asphalt covering is widely used in road construction due to its smooth jointless cover, driving comfort, and fast installation. Asphalt covers are sensitive to two main types of influences: mechanical loads, especially heavy vehicles, and meteorological impacts due to changes in humidity, temperature, and freeze–thaw cycles [32].

Moreover, a new asphalt cover, even in the absence of traffic load or other artificial activities, degrades due to meteorological and environmental factors [33]. Fatigue, cold temperatures, and wear-out cracks are the main problems for road covers. In recent years, thermal cracks and low-temperature destruction have become key factors researched for asphalt covers in cold regions, as road covers' lifetimes decrease due to freezing and thawing cycles in cold geographical zones. Freezing–thawing cycles are considered the biggest weather trigger for road deformation [34–36]. During the cycle, the environmental temperature repeatedly changes from positive to negative and the road cover suffers from frequent thermal stress and moisture influences.

Furthermore, the components of an asphalt cover degrade due to environmental factors such as temperature, solar radiation, water, and air [37]. As asphalt is a viscoelastic material, temperature is one of the main factors that impact it. It is well known that asphalt is liable to flow at high temperatures and to break down at low temperatures.

Researchers from China have proposed preventing huge amounts of road destruction by predicting a road's state on the basis of soil moisture variables as the main underlying factor of deformation [38]. Moisture's negative effect on a road's state has been experimentally demonstrated in South Korea [39].

The environmental factors considered should also include the landscape dynamics, which are affected by meteorological characteristics. The main meteorological factors that we consider should be chosen with regard to the trigger mechanisms of landslide pro-

cesses [40]. Water's effect on slope failure has been shown via simulation and experimental tests [41,42]. Landslide forecasting is dependent on rainfall data, time period, and the size of the geographical location [43]. In a study on the relationship between rainfall and landslide intensity, the duration and previous amounts of rainfall were mainly used [12]. However, snow melting and long spells of non-intensive fallouts can have a significant impact, as they lead to an increase in the ground water level, and short but intensive rainfall can lead to the migration of humidification fronts and to pressure changes in interstitial water. Extreme rainfall phenomena strongly affect the beginning of landslide processes.

The abovementioned results highlight the necessity of using complex meteorological data for automobile road state diagnostics to find both direct and indirect correlations.

Thus, the following meteorological characteristics should be considered:

1. Extremely high temperatures (above 30 °C);
2. Extremely low temperatures (less than −15 °C);
3. Freezing and thawing cycles;
4. Solar radiation;
5. Air humidity;
6. Highly intensive rainfall (more than 30 mm in 3 h);
7. Long but non-intensive rainfall.

As was discussed in Section 2.1 regarding the republic's geographical region, all three temperature factors are relevant. Solar radiation and air humidity should be considered too, as the atmosphere is dry. Fallouts are usually rare but intensive, meaning that the last factor can be ignored.

However, the project's goal requires open access meteorological data for the region that cover the last several years. Therefore, data from the <http://meteocenter.net/> (accessed on 1 April 2021) internet resource were chosen as the main source of archival meteorological data. The data regarding temperature and rainfall amount are accessible at 3 h time intervals from March of 2005, which is very convenient for our computations. The temperature data help us to consider the direct impacts of heating and cooling on the asphalt road cover. The rainfall amount allows us to study the landslide processes caused by the soil moisture increase and rain, snow, or ice's impact on the road cover. Data on air humidity were downloaded from the archive too. Unfortunately, solar radiation values are absent from the archive. However, they can be indirectly calculated from the cloudiness value. The solar radiation data for the project were obtained via remote sensing methodologies.

3.3. Remotely Sensed Parameter Choice

The choice of the parameters identified via satellite images was made according to the results of research on landslide processes' origins (of unknown type and size), which can be summarized as:

- Terrain amplitude rise and height decrease at the highest point (i.e., in the source or depletion region);
- Reduction in both amplitude and height at the base of a landslide deposit;
- Growth of amplitude and height in a lower part (i.e., setting zone) [44].

The recommendations are to provide a landscape inventory by comparing images from different periods. Hill slope, aspect, contour, and shading maps were designed. These datasets were then combined with satellite images over time with a high resolution to depict current and potential dynamic zones.

After taking into account the scientific literature, the field research, discussions with the project team, and the accessibility of the satellite images, the following parameters were chosen for remote sensing:

1. Vertical displacements with coherent points;
2. Slope exposure;
3. Dissections;
4. Topographic wetness index;

5. Aspect;
6. Solar radiation;
7. Vegetation index SAVI;
8. Snow-covered zones.

The first five parameters describe the landscape dynamics from different perspectives. The topographical humidity index, solar radiation, vegetation index SAVI, and snow-covered zones detect additional environmental factors.

The processing of 149 archive images from the Sentinel-1 satellite from 2017–2021 resulted in the creation of maps for the geodynamical assessment of the automobile road territory. More can be read about the image processing methodology and instruments in the authors' past article [45].

4. Results and Discussion

4.1. Road's Deformation Data

The road laboratory provided a visual examination of the Almaty–Cosmostation road according to the abovementioned standards on 19 May 2021. The results are presented in Table 2 per kilometer of the road.

Table 2. Results of visual examination of the Almaty–Cosmostation road.

Number of the Road km	Road Width, m	Score According to [30]	Details
1	9.5	I/1	No deformation registered.
2	9.5	I/1	No deformation registered.
3	9.5	I/1	No deformation registered.
4	9.5	I/1	No deformation registered.
5	8.0	I/1	No deformation registered.
6	8.0	I/1	No deformation registered.
7	8.0	I/1	No deformation registered.
8	8.0	I/1	No deformation registered.
9	7.5	I/3	Transverse cracks and unevenness.
10	7.5	I/2–3	Transverse cracks and unevenness.
11	7.5	I/2–3	Transverse cracks and unevenness.
12	7.5	I/3–4	Transverse cracks and unevenness.
13	7.5	I/4	Transverse cracks and unevenness.
14	–	–	Construction work. No traffic.
15	–	–	Construction work. No traffic.
16	–	–	Construction work. No traffic.
17	7.2	I/1–2	New roadbed. Some transverse cracks at 2–3 m intervals
18	7.2	I/2	New roadbed. Some transverse cracks at 2–3 m intervals
19	7.2	I/4	Clear longitudinal and transverse cracks. Occasional crack network. Washed out road slope (WoS).
20	7.2	I/4	Clear longitudinal and transverse cracks. Occasional crack network.
21	7.2	II	Clear longitudinal and transverse cracks. Occasional crack network.

According to the results shown in Table 1, the road cover at the beginning of the road from Al-Farabi Street up to 8 km is in great condition. There are no pronounced defects. The road's width varies between 8.5 and 9 m. Further, at the 9th kilometer, the roadway narrows to 7.5 m. Transverse and longitudinal cracks, small holes (SH), and small crack networks rarely appear. Construction work is being conducted from the 14th kilometer for 3 km. This sector is restricted for almost all traffic. The final quarter of the road starting from the 17th kilometer has a width of only 7.2 m and has been damaged the most. As the height grows, both longitudinal and transverse cracks become bigger and form crack networks. Even some substantial roadbed destruction appears.

Consequently, the road laboratory staff chose five 50 m testing sections at the 18th and 19th kilometers for more detailed diagnostics on the same date (19 May 2021) (Figure 2).

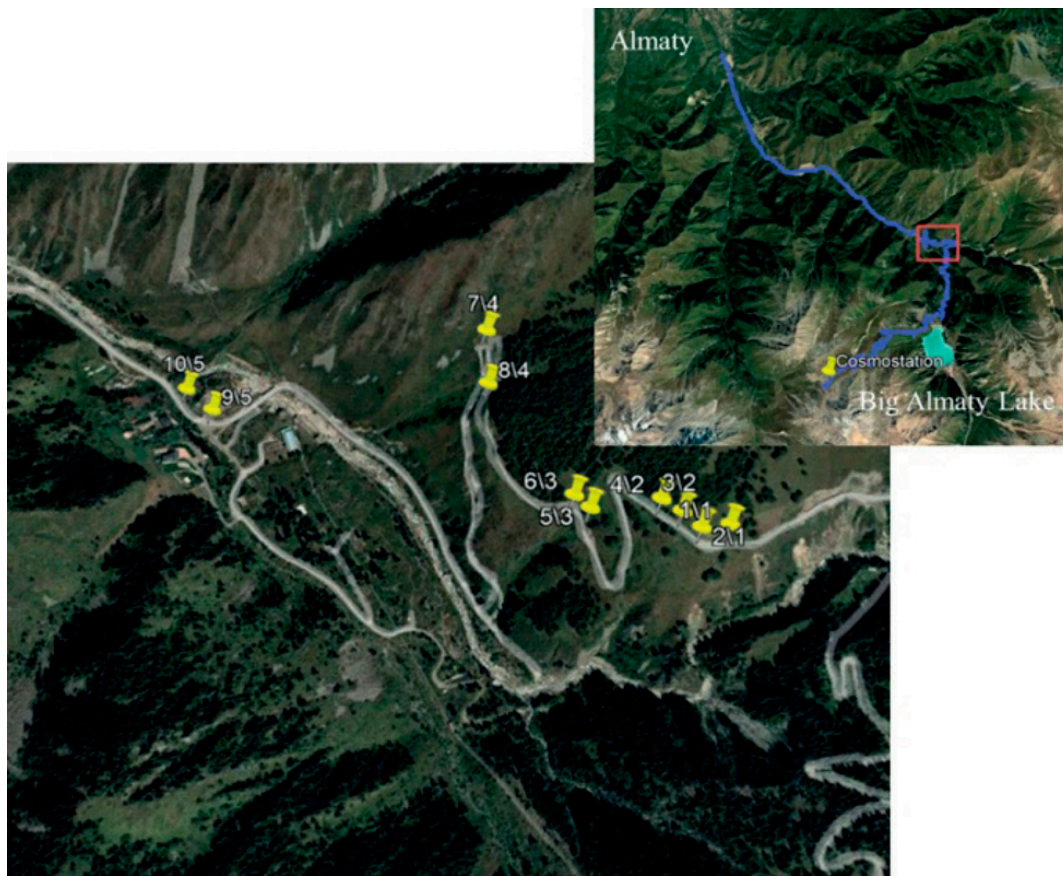


Figure 2. The testing sections on the Almaty–Cosmostation road, where numbers before and after “/” sign identify the point and section numbers consequently.

Each section is identified by a yellow mark in Figure 2. The highest section, identified as 1/1 and 2/1, has a small grade, and the road widens over the hill’s slope. The second section, between 3/2 and 4/2, has a bigger grade, and the width is normal for this part of the road. The third section (5/3 and 6/3) differs from the second, as it has a slightly smaller grade and is wider. The section marked as 7/4 and 8/4 is the narrowest of all five. It is different due to the hill’s slope on its sides and the critical deformations in the roadbed. The last section (9/5 and 10/5) was chosen as a reference section, as it passes over an almost flat landscape and is visually unaffected by geological triggers. The detailed diagnostics results are presented in Table 3 for each testing section.

Table 3. Detailed diagnostics results of the testing sections.

Testing Section	Transversal Crack by Length					Total Length, m	Longitudinal Crack, m			Total Length, m	Crack Network	Details
	0–1 m	1–2 m	2–3 m	3–4 m	4–5 m		On a Left Side	In a Center	On a Right Side			
1/1–2/1	6	3	1	-	-	15	Σ11.5	Σ16.9	Σ12.1	41	2	-
3/2–4/2	8	3	2	-	-	20	Σ8	Σ17.04	Σ13.9	39	5	-
5/3–6/3	7	6	3	2	-	36	Σ17.8	Σ19.25	Σ7.4	44	3	-
7/4–8/4	11	6	3	3	1	49	Σ34.8	Σ3.3	Σ22.2	60	2	Washed out road slope (WoS)
9/5–10/5	5	4	2	1	1	28	Σ6.8	Σ18.1	Σ15.6	41	2	Small holes (SH)

The worst road state is in the fourth section, which has a washed-out road slope and the greatest amount of all crack types, except central longitudinal cracks and crack networks. The third section is in a much better situation both in terms of individual cracks and total

length, while the crack networks are slightly bigger than for the fourth one. Sections one and two are in the best situation in terms of the total number of transversal and longitudinal cracks, although the second sector has the greatest number of crack networks. Surprisingly, the fifth section is similar to the others in terms of longitudinal cracks and crack networks, but it has long transversal cracks and even small holes in its cover.

4.2. Factual Meteorological Data

All meteorological data were downloaded from the open source meteorological archive at <http://meteocenter.net/> (accessed on 1 April 2021) as six Excel files covering January 2016 to March 2021. Each file contains a different list for each month, where one time slot lies on one or more line (meaning that some lines are arguably empty). In addition, not all the data are relevant to the project's goals, as was discussed previously. The program required to download the data and form and clean the Excel files was written by means of Python programming language. The following data were downloaded:

1. Horizontal visibility at a 2 m level above the Earth's surface, m;
2. Natural phenomena names;
3. Natural phenomena amount, mm;
4. Basic cloudiness, %;
5. Low level cloudiness (lower than 2000 m), %;
6. Air temperature, °C;
7. Air humidity, %;
8. Rainfall, mm;
9. Snow cover, cm.

The air temperature, humidity, rainfall, and snow cover were considered to be the main triggers of deformation. The horizontal visibility and two types of cloudiness could be used as indirect indicators of solar radiation affecting the road cover's state. The data concerned natural phenomena detailed rainfall and air characteristics. All the downloaded data are accessible in the open database of the project. The extracted values are listed in Table 4.

Table 4. Factual meteorological data.

Year	Extremely High Temperature (>30 °C), Number of 3 h Periods	Extremely Low Temperature (<−15 °C), Number of 3 h Periods	Freezing and Thawing Cycles, Number	Air Humidity (Min–Max), %	Highly Intensive Rainfall Values (More Than 30 mm un 3 h), Number of Periods	Rainfall/Snow Cover Maximum Value, mm/cm
2016	62	1	102	0–100	10	43/42
2017	130	0	151	0–100	4	701/598
2018	107	60	93	0–100	0	26/25
2019	133	1	133	13–100	2	45/33
2020	76	0	105	0–100	3	320/598
First 3 month of 2021	0	11	63	16–96	0	21/23

The meteorological data for the road's region shows that extremely high temperatures and freezing–thawing cycles are frequent, as is true all across the republic. Extremely low temperatures, however, happen only in particular years. Rainfall is irregular but tremendously intensive.

Winter is characterized by extremely low temperatures, fairly high humidity, the lowest level of rainfall, high snow cover, and regular freeze–thaw cycles. Spring is characterized by freeze–thaw cycles, low temperatures, some snow cover at the beginning, and the highest intensity of rain. Extreme high temperatures, low humidity, extensive rainfall, and some freeze–thaw cycles characterize the summer. Fall is similar to spring, except for fallouts and snow cover, which show the reverse trends.

As the meteorological characteristics are typical for the road’s region, they presumably influence the road cover similarly at all the testing sections. Hence, their impacts result in similar destruction patterns (nearly 40 m of total longitudinal cracks, 15 m of total short transversal cracks, and two crack networks for road sections of 50 m). Larger deformations are aligned with the individual landscape characteristics of the sections.

4.3. Correlation between Landscape and Road Deformation Data

One of the main questions of the article is whether the remotely sensed parameters regarding the landscape can be used to calculate the road’s deformation level. That is to say, is there any sufficient correlation between the previously listed characteristics and the road state? To research this correlation, the road characteristics from Table 3 are summarized using three values:

1. Total length of transversal cracks;
2. Total length of longitudinal cracks;
3. Essential destruction (SH—small holes, WoS—washed out slope).

These values were added to the figures representing remotely sensed parameters in Figures 3–9 using red or yellow text near each testing section of the road.

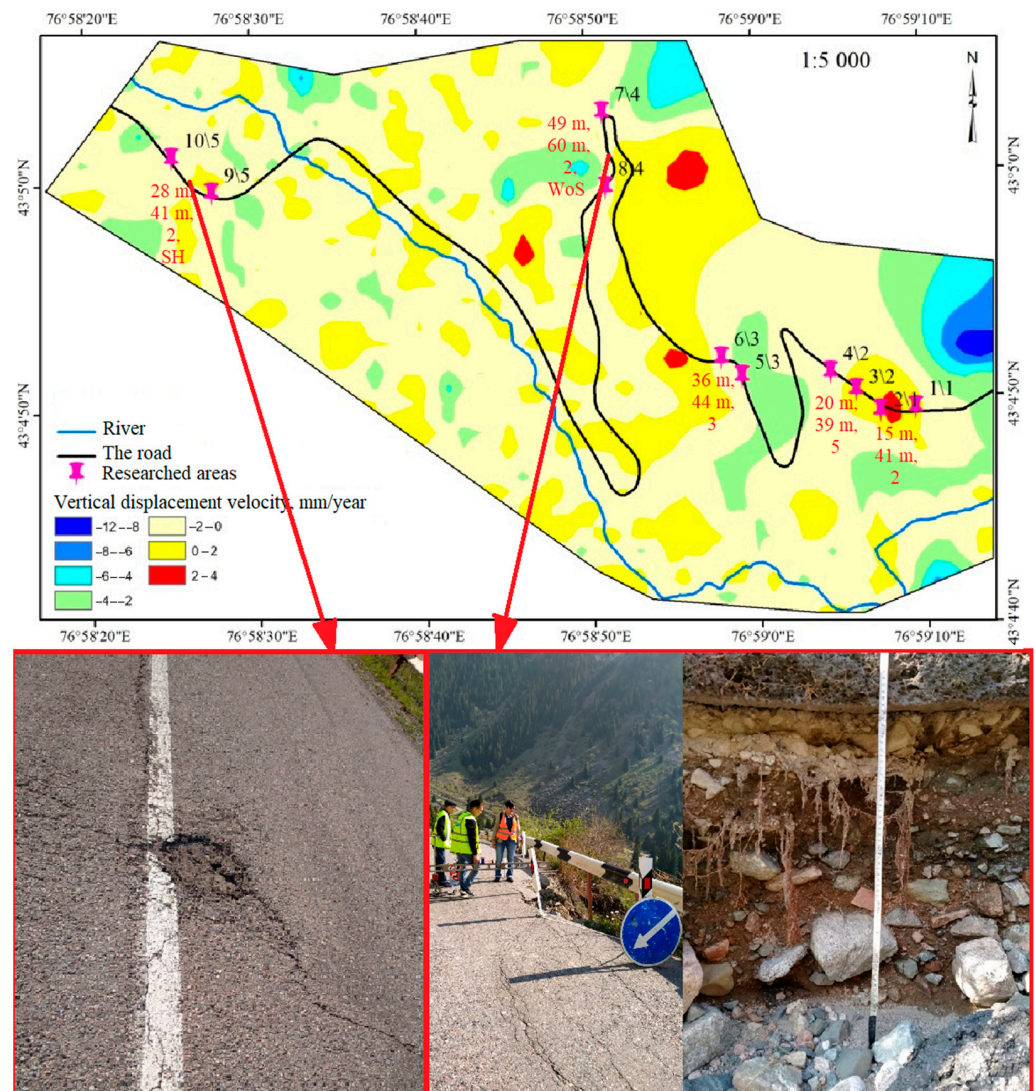


Figure 3. Vertical displacement velocity compared with the road state (red text on above and photos at the bottom) at each testing section (pink marks).

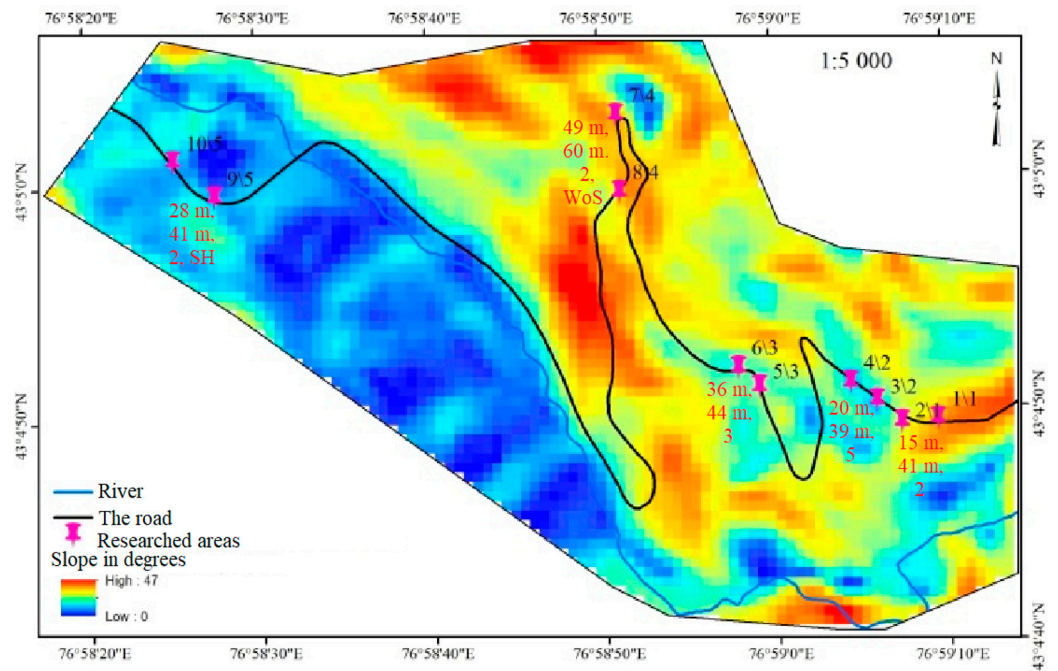


Figure 4. Slope degrees compared with the road’s state (red text) at each testing section (pink marks).

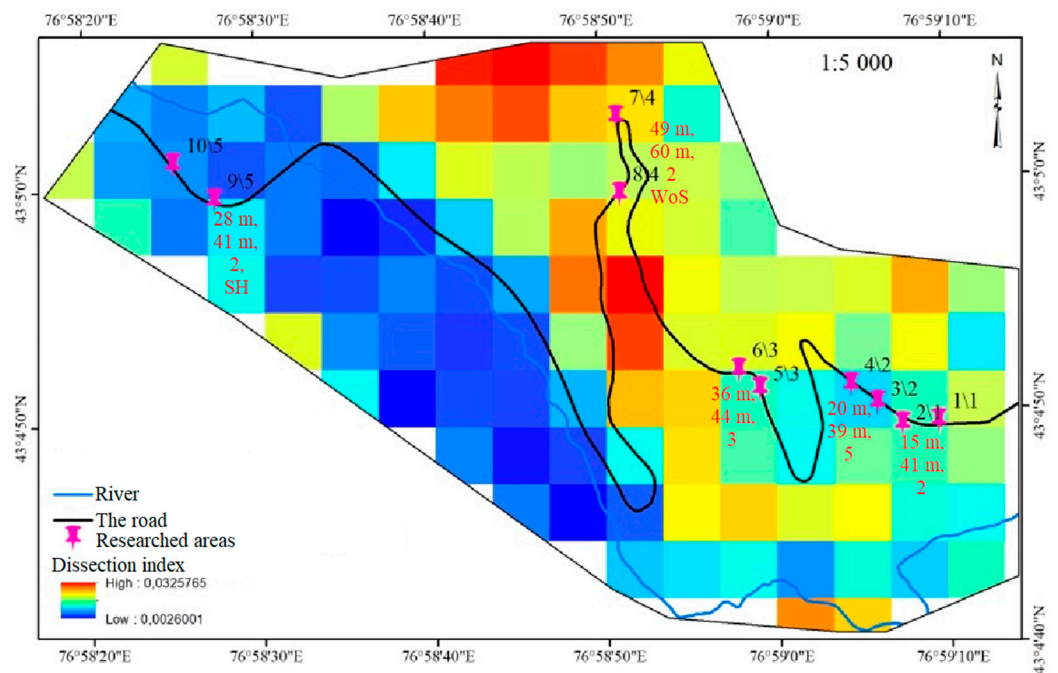


Figure 5. Dissection index compared with the road’s state (red text) at each testing section (pink marks).

The parameter that indicated the landscape dynamics the most is the vertical displacement velocity. Positive velocity values show the upper movement of the surface, while negative values show failures. The value describes the intensity of the movement. The vertical displacement velocity of the road’s area is shown in Figure 3.

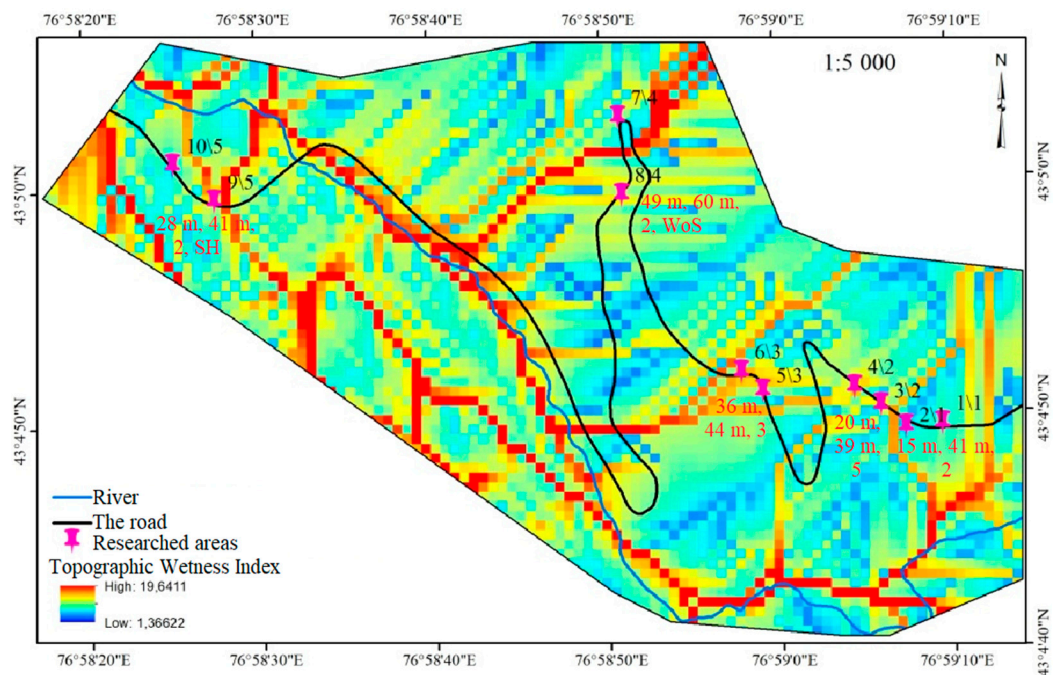


Figure 6. Topographic wetness index compared with the road’s state (red text) at each testing section (pink marks).

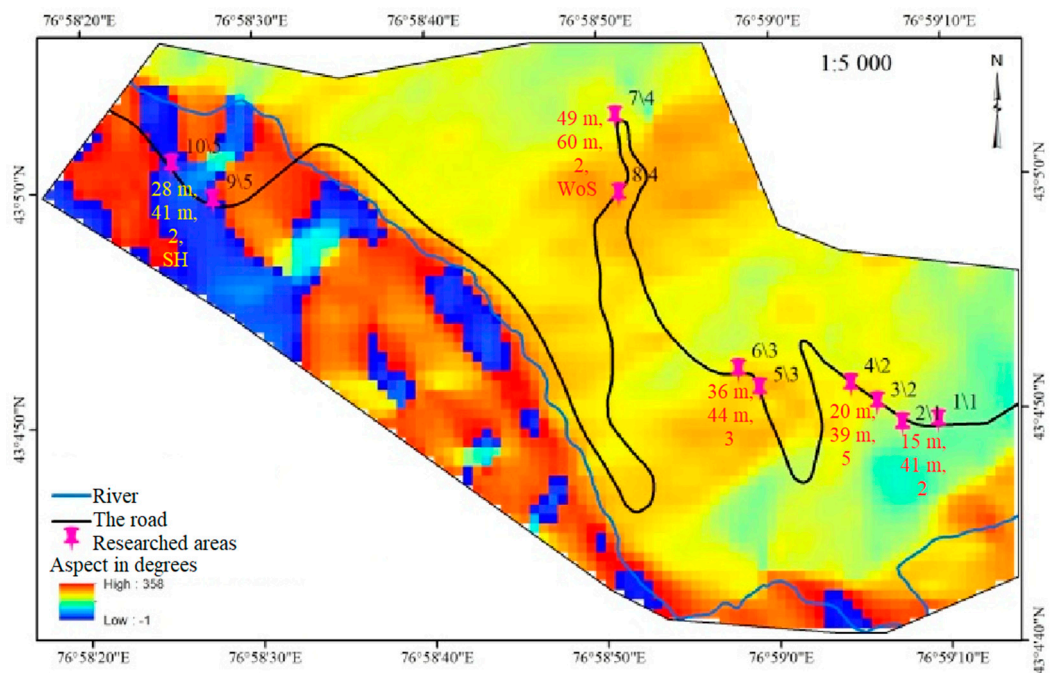


Figure 7. Aspect of the slope in degrees compared with the road’s state (red and yellow text) at each testing section (pink marks).

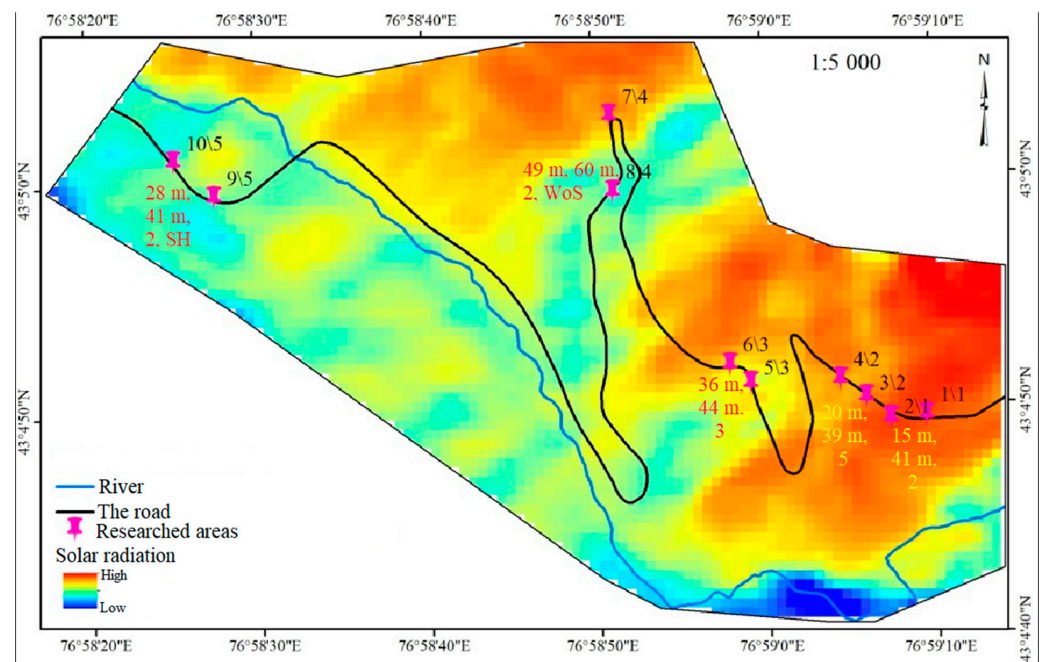


Figure 8. Solar radiation compared with the road’s state (red and yellow text) at each testing section (pink marks).

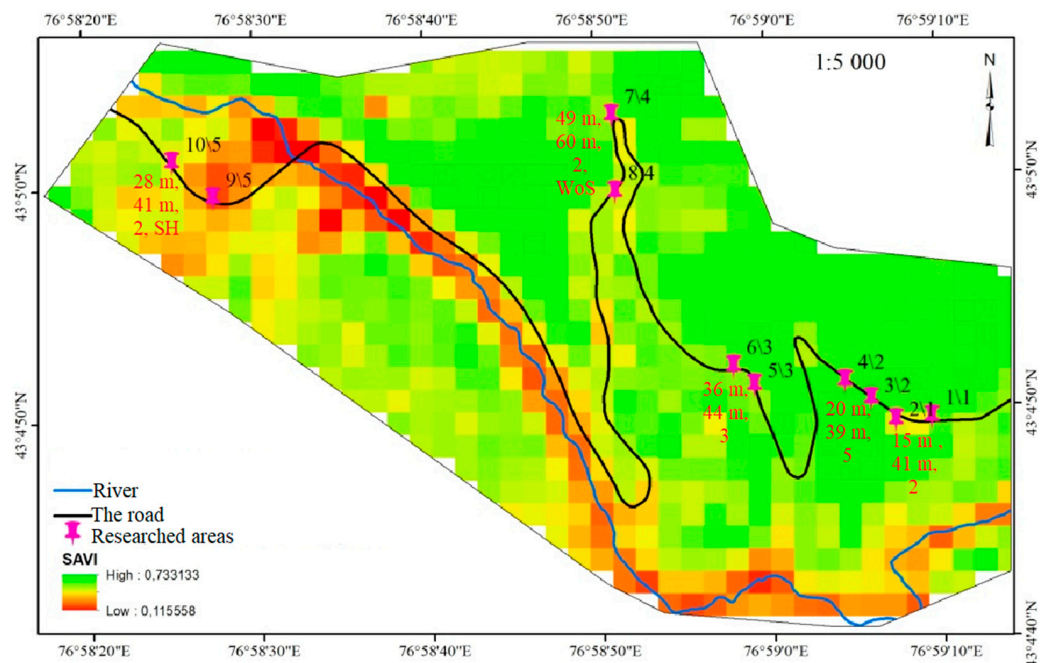


Figure 9. Vegetation index SAVI compared with the road’s state (red text) at each testing section (pink marks).

The landscape’s active movement directly interferes only with one testing section of the road—the first one (between 1/1 and 2/1). It lies in the fast-growing area, which is shown in red. Three sections (3/2–4/2, 5/3–6/3, and 7/4–8/4) pass between landscapes with movement in different directions (red—growing; blue and green—falling). The difference between the vertical displacement velocities is more noticeable for the fourth section, which has the worst state in every sense except number of crack networks. Interestingly, the longitudinal cracks in this section are mainly present on the sides, but not in the middle of the road. The last section (9/5–10/5) has almost no movement of the landscape. These data

suggest that a large parallel or vertical displacement velocity applied to a road section is not as disruptive as perpendicular differences in velocity.

Road constructors measure such a landscape parameter in slope degrees. Therefore, its correlation with the road state should be considered as well (Figure 4).

Predictably, high slope values characterize the first (1/1–2/1) and fourth (7/4–8/4) sections. The other three sections pass places with below-average slope degrees. This means that no significant correlation is visible.

The next parameter to consider is the dissection index. This landscape characteristic is compared with the road state in Figure 5.

The locations of the highest dissection indexes do not match any of the testing sections. The road passes one of the zones with the highest dissection index twice—before and after the fourth section (7/4–8/4). This means that the road deformation does not have a significant impact on the road state. However, the dissection index of the testing section with the worst characteristics (7/4–8/4) is higher than the average. The best dissection index is found for the section with essential deformation in the form of small holes (9/5–10/5).

The landslide dynamics could be triggered by soil reduction caused by water flows or wetness levels. Accordingly, the topographic wetness index is considered in Figure 6.

The highest index coincides with the essential deformation of the road pavement, including the washing out (WoS) in the fourth section (7/4–8/4) and the small holes (SH) in the last section (9/5–10/5). However, a considerable part of the road between these two sections passes alongside the high topographic wetness index line and even passes through it without showing any significant destruction. The other sections are in locations with near-average index values.

The aspect of the slope indicates both internal and external landscape characteristics. It is an indirect indicator of the environmental triggers of landslide processes and road destruction such as solar radiation, vegetation characteristics, and the snow melting process. Its visualization in the context of the road regions is shown in Figure 7.

The third (5/3–6/3) and fourth (7/4–8/4) sections have the highest aspects. The second section (3/2–4/2) is in an area with a slightly lower aspect. The first section (1/1–2/1) has an average aspect value. The fifth section (9/5–10/5) has the lowest aspect. The aspect does not demonstrate any direct correlation with the road's state. Therefore, the research group decided to consider solar radiation directly from the satellite images (Figure 8).

According to Figure 8, the first two sections (1/1–2/1 and 3/2–4/2) are the most affected by solar radiation. The third section (5/3–6/3) is impacted too, but to a lower degree. The fourth section has mixed effects from the sun and shows high-level radiation at the high point and a much lower level at the bottom. The last section (9/5–10/5) is negligibly influenced by solar radiation. One might assume that solar radiation affects the number of longitudinal cracks in the first and second sections by triggering the displacement of road pavement. However, such a dynamic would cause a greater amount of transversal cracks in section four, which was not observed.

The second external factor to consider is the vegetation index SAVI, which is shown in Figure 9. This parameter represents a numerical measure of both plant and soil types.

SAVI is moderately high for all the testing sections except the last one (9/5–10/5), which has a vegetation index below average. However, as with the topographic wetness index, a large part of the road cover passes nearby areas of low SAVI.

The last factor to be considered in the article is snow cover throughout the researched period. It is a dynamic factor, which is hardly possible to visualize on one or a number of figures. Therefore, to show the extreme changes in snow cover in different seasons, Figure 10 for winter and Figure 11 for spring are provided.

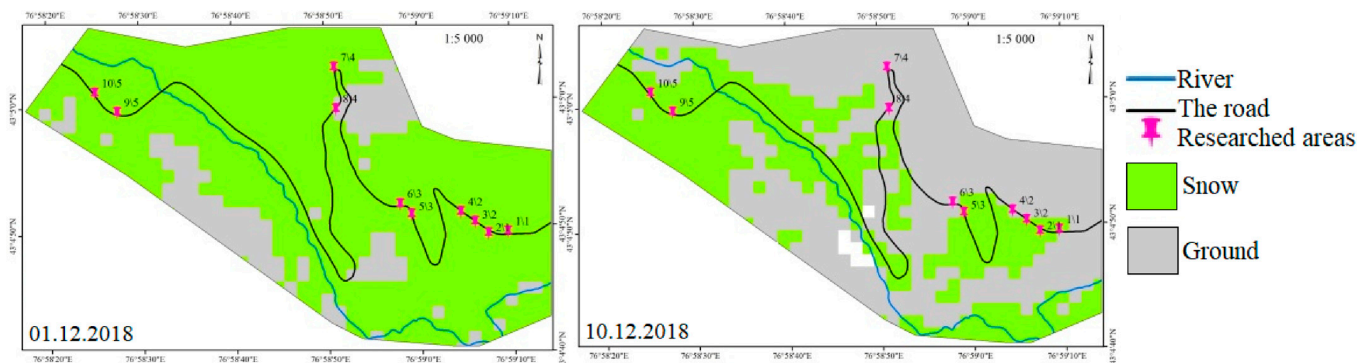


Figure 10. Snow cover difference at the beginning of the winter of 2018–2019.

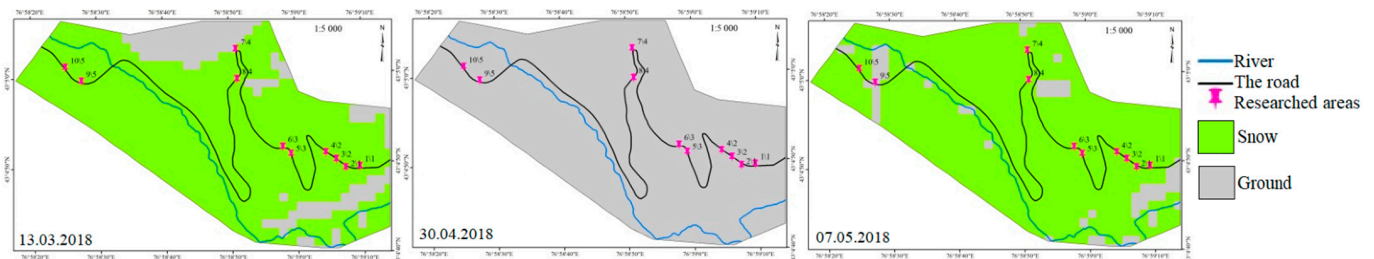


Figure 11. Snow cover difference in spring 2018.

In both examples, the last to lose the snow cover are first three sections (1/1–2/1, 3/2–4/2 and 5/3–6/3). Snow melting starts just above the fourth section (7/4–8/4), and the lower side retains the cover longer. The fifth section (9/5–10/5) loses snow cover faster than other sections (Figure 11) or preserves slow-melting areas (Figure 10). The snow-melting process correlates with the essential destruction of the road.

Our comparison of the remotely sensed parameters and road state shows that:

1. The first testing section is negatively affected by high vertical displacement velocity, high slope values, and solar radiation; its aspect is average; and its topographic wetness index is very low;
2. The second testing section of the road is negatively affected by a moderate parallel difference of vertical displacement velocities and a high aspect and solar radiation, but the slope value and topographic wetness index are average;
3. The third testing section of the road is negatively affected by a moderate parallel difference of vertical displacement velocities and the highest aspect, but the slope value, topographic wetness index, and solar radiation are average;
4. The fourth testing section of the road is negatively affected by a high perpendicular difference of vertical displacement velocities, a high slope, a relatively high dissection index value, a high topographic wetness index, the highest aspect, and snow-melting, but its solar radiation is mixed;
5. The fifth testing section of the road is negatively affected by a high topographic wetness index, SAVI, and snow melting, but its vertical displacement velocity and slope values are average and its dissection index, aspect, and solar radiation are very low.

To summarize the comparison, all the remotely sensed parameters affect the road's state with different intensities, causing various types of destruction. Hence, remotely sensed landscape information can be used for remote automobile road diagnostics.

5. Conclusions

Local demand for remote road diagnostics and forecasting methodologies based on open source data has increased due to the huge road distances and significantly low popu-

lation density of the Republic of Kazakhstan. Its roads are exposed to severe meteorological changes and landscape complexities.

The theoretical assumption was that timely automobile road diagnostics are possible to make by processing open data from remote sensing and meteorological archives. To verify this assumption, the authors compared the results of road diagnostics via road laboratory and ground-penetrating radar with data from meteorological archives and remote sensing from cosmic images near the automobile road.

The meteorological data were downloaded from an open source meteorological archive (<http://meteocenter.net/> (accessed on 1 April 2021)) covering January 2016 to March 2021. Extremely high temperature ($>30\text{ }^{\circ}\text{C}$) varies from 62 to 133 days per year, extremely low temperature ($<-15\text{ }^{\circ}\text{C}$) varies from 0 to 60 days per year, freezing and thawing cycles vary from 93 to 151 per year, rainfall and snow cover maximum value vary from 26 mm and 25 cm to 701 mm and 598 cm per year, respectively. Thus, meteorological data for the road's region show that extremely high temperatures, frequent freezing–thawing cycles, and irregular, intensive rainfall are common. Extremely low temperatures, however, only occur in some years.

The impact of these phenomena leads to road destruction, which amounts to nearly 40 m of total longitudinal cracks and 15 m of total short transversal cracks forming two crack networks on average for a road section of 50 m. Larger deformations are aligned with the individual landscape characteristics of the testing section.

A total of 149 open access archive images from Sentinel-1 satellite over the period 2017–2021 were processed to form a pool of remote sensing data. A comparative analysis of the correlations between the road's state and remotely sensed parameters is shown in Table 5.

Table 5. Comparison between road's state and remotely sensed parameters.

Testing Section	Total Length of Transversal Crack, m/Total Length of Longitudinal Crack, m/Crack Network, Number/Details	Vertical Displacement Velocity	Slope Exposure	Dissections	Topographic Wetness Index	Aspect	Solar Radiation	Vegetation Index SAVI	Snow-Melting
1/1–2/1	15/41/2	++ ¹	++	-	-	-	++	-	-
3/2–4/2	20/39/5	±	-	-	-	+	++	-	-
5/3–6/3	36/44/3 49/60/2/	±	-	-	-	++	-	-	-
7/4–8/4	Washed out road slope	++	++	+	++	++	±	-	+++
9/5–10/5	28/41/2/Small holes	-	-	-	++	-	-	++	++
Other parts of road	-	+	++	+++	++	-	++	++	+++

¹ “+” sign means a growth, “-” sign means a fall, both signs mean some combination of growth and fall where a standing order describes position with respect to the road direction.

The testing section with the worst road state (the fourth section) suffers from the negative effects of all considered parameters except vegetation index SAVI. SAVI affects the fifth section alongside a high topographic wetness index and the snow-melting process, causing essential deformation of the road cover (small holes). The other three sections are affected by several parameters in different combinations, leading to smaller but essential deformations of the road. All the negative factors influenced the other parts of the road, resulting in a 1/4 overall value of the road's state (as was described in Section 3.1 of the article).

These findings confirm the previously stated assumption that automobile road diagnostics are possible to make by processing open access data from remote sensing and meteorological archives.

The processed data forming the database will be used to train several types of intellectual prediction models in the next stage of the research. Moreover, the correlations will be confirmed or disposed of by the weighting values of future intellectual models.

Data received from the meteorological archive, satellite images, and additional field research in 2022–2023 will be uploaded to the database within the next two years. The database is open for any research purposes at <http://ionos.kz/intellsystlandslide/> (accessed on 1 November 2022).

Author Contributions: Conceptualization, A.K., G.N. and D.P.; methodology, G.N., Z.Z., R.S., D.P. and S.K.; software, D.P. and K.P.; validation, A.K., G.N., R.S., D.P. and S.K.; formal analysis, A.K., G.N. and D.P.; investigation, A.K., G.N., R.S., D.P., S.K. and K.P.; resources, G.N., D.P. and K.P.; data curation, G.N., D.P. and K.P.; writing—original draft preparation, A.K., G.N., D.P. and K.P.; writing—review and editing, A.K., G.N. and D.P.; visualization, G.N. and D.P.; supervision, A.K. and Z.Z.; project administration, A.K. and Z.Z.; funding acquisition, A.K. and Z.Z. All authors have read and agreed to the published version of the manuscript.

Funding: This research is funded by the Science Committee of the Ministry of Science and Higher Education of the Republic of Kazakhstan (Grant No. AP09260066).

Data Availability Statement: The data presented in this study are openly available at <http://ionos.kz/intellsystlandslide/> (accessed on 1 November 2022).

Conflicts of Interest: The authors declare no conflict of interest.

References

- Gkyrtis, K.; Plati, C.; Loizos, A. Mechanistic Analysis of Asphalt Pavements in Support of Pavement Preservation Decision-Making. *Infrastructures* **2022**, *7*, 61. [\[CrossRef\]](#)
- Mičechová, L.; Mikolaj, J.; Šedivý, Š. New knowledge in the field of the diagnostic and evaluation of selected pavement parameters. *Transp. Res. Procedia* **2019**, *40*, 373–380. [\[CrossRef\]](#)
- Staniek, M.; Czech, P. Self-correcting Neural network in road pavement diagnostics. *Autom. Constr.* **2018**, *96*, 75–87. [\[CrossRef\]](#)
- Kheirati, A.; Golroo, A. Low-cost infrared-based pavement roughness data acquisition for low volume roads. *Autom. Constr.* **2020**, *119*, 103363. [\[CrossRef\]](#)
- Đurinová, M.; Mikolaj, J. Definition of pavement performance models as a result of experimental measurements. *Transp. Res. Procedia* **2019**, *40*, 201–208. [\[CrossRef\]](#)
- Oreto, C.; Massotti, L.; Biancardo, S.A.; Veropalumbo, R.; Viscione, N.; Russo, F. BIM-Based Pavement Management Tool for Scheduling Urban Road Maintenance. *Infrastructures* **2021**, *6*, 148. [\[CrossRef\]](#)
- Braunfelds, J.; Senkans, U.; Skels, P.; Janeliukstis, R.; Porins, J.; Spolitis, S.; Bobrovs, V. Road Pavement Structural Health Monitoring by Embedded Fiber-Bragg-Grating-Based Optical Sensors. *Sensors* **2022**, *22*, 4581. [\[CrossRef\]](#)
- Al-Mansour, A.I.; Al-Qaili, A.H. An Application of Android Sensors and Google Earth in Pavement Maintenance Management Systems for Developing Countries. *Appl. Sci.* **2022**, *12*, 5636. [\[CrossRef\]](#)
- Zhantayev, Z.; Kairanbayeva, A.; Kiyalbayev, A.; Nurpeissova, G.; Panyukova, D. Data collection for intellectual forecasting: Methods and results. *News Natl. Acad. Sci. Repub. Kazakhstan. Ser. Phys.-Math.* **2021**, *4*, 108–117. [\[CrossRef\]](#)
- Steger, S.; Mair, V.; Kofler, C.; Pittore, M.; Zebisch, M.; Schneiderbauer, S. Correlation does not imply geomorphic causation in data-driven landslide susceptibility modelling—Benefits of exploring landslide data collection effects. *Sci. Total Environ.* **2021**, *776*, 145935. [\[CrossRef\]](#)
- Intrieri, E.; Carlà, T.; Gigli, G. Forecasting the time of failure of landslides at slope-scale: A literature review. *Earth-Sci. Rev.* **2019**, *193*, 333–349. [\[CrossRef\]](#)
- Chikalamo, E.E.; Mavrouli, O.C.; Ettema, J.; van Westen, C.J.; Muntohar, A.S.; Mustofa, A. Satellite-derived rainfall thresholds for landslide early warning in Bogowonto Catchment, Central Java, Indonesia. *Int. J. Appl. Earth Obs. Geoinf.* **2020**, *89*, 102093. [\[CrossRef\]](#)
- Li, M.; Zhang, L.; Ding, C.; Li, W.; Luo, H.; Liao, M.; Xu, Q. Retrieval of historical surface displacements of the Baige landslide from time-series SAR observations for retrospective analysis of the collapse event. *Remote Sens. Environ.* **2020**, *240*, 111695. [\[CrossRef\]](#)
- Mondini, A.C.; Guzzetti, F.; Chang, K.-T.; Monserrat, O.; Martho, T.R.; Manconi, A. Landslide failures detection and mapping using Synthetic Aperture Radar: Past, present and future. *Earth-Sci. Rev.* **2021**, *216*, 103574. [\[CrossRef\]](#)

15. Bondur, V.; Chimitdorzhiev, T.; Dmitriev, A.; Dagurov, P. Fusion of SAR Interferometry and Polarimetry Methods for Landslide Reactivation Study, the Bureya River (Russia) Event Case Study. *Remote Sens.* **2021**, *13*, 5136. [CrossRef]
16. Teshebaeva, K.; Roessner, S.; Ehtler, H.; Motagh, M.; Wetzel, H.-U.; Molodbekov, B. ALOS/PALSAR InSAR Time-Series Analysis for Detecting Very Slow-Moving Landslides in Southern Kyrgyzstan. *Remote Sens.* **2015**, *7*, 8973–8994. [CrossRef]
17. Pfurtscheller, C.; Genovese, E. The Felbertauern landslide of 2013 in Austria: Impact on transport networks, regional economy and policy decisions. *Case Stud. Transp. Policy* **2019**, *7*, 643–654. [CrossRef]
18. Zhang, Q.; Yu, H.; Li, Z.; Zhang, G.; Ma, D.T. Assessing potential likelihood and impacts of landslides on transportation network vulnerability. *Transp. Res. Part D Transp. Environ.* **2020**, *82*, 102304. [CrossRef]
19. Leonardi, G.; Palamara, R.; Suraci, F. A fuzzy methodology to evaluate the landslide risk in road lifelines. *Transp. Res. Procedia* **2020**, *45*, 732–739. [CrossRef]
20. Sarychikhina, O.; Palacios, D.G.; Argote, L.A.D.; Ortega, A.-G. Application of satellite SAR interferometry for the detection and monitoring of landslides along the Tijuana—Ensenada Scenic Highway, Baja California, Mexico. *J. S. Am. Earth Sci.* **2021**, *107*, 103030. [CrossRef]
21. Lee, C.-F.; Huang, W.-K.; Chang, Y.-L.; Chi, S.-Y.; Liao, W.-C. Regional landslide susceptibility assessment using multi-stage remote sensing data along the coastal range highway in northeastern Taiwan. *Geomorphology* **2018**, *300*, 113–127. [CrossRef]
22. Nappo, N.; Peduto, D.; Mavrouli, O.; van Westen, C.J.; Gullà, G. Slow-moving landslides interacting with the road network: Analysis of damage using ancillary data, in situ surveys and multi-source monitoring data. *Eng. Geol.* **2019**, *260*, 105244. [CrossRef]
23. Official Website of the President of the Republic of Kazakhstan. Available online: https://www.akorda.kz/ru/republic_of_kazakhstan/kazakhstan (accessed on 1 September 2022).
24. Central Asian Countries Geoportal. Available online: <https://cac-geoportal.org/> (accessed on 3 September 2022).
25. Kazakhstan Climate Zone, Weather by Month and Historical Data. Available online: <https://tckctck.org/kazakhstan> (accessed on 18 November 2022).
26. Agency for Strategic Planning and Reforms of the Republic of Kazakhstan Bureau of National Statistics. Express Information. Available online: <https://stat.gov.kz/official/industry/61/statistic/6> (accessed on 3 September 2022).
27. Automobile Road’s Length. Available online: <https://stat.gov.kz/api/getFile/?docId=ESTAT099963&lang=ru> (accessed on 29 August 2022).
28. Pantuso, A.; Loprencipe, G.; Bonin, G.; Teltayev, B.B. Analysis of Pavement Condition Survey Data for Effective Implementation of a Network Level Pavement Management Program for Kazakhstan. *Sustainability* **2019**, *11*, 901. [CrossRef]
29. Bonin, G.; Folino, N.; Loprencipe, G.; Oliverio Rossi, G.; Polizzotti, S.; Teltayev, B. Development of a Road Asset Management System in Kazakhstan. In Proceedings of the TIS 2017 International Congress on Transport Infrastructure and Systems, Rome, Italy, 10–12 April 2017; pp. 10–12.
30. PR RK 218-27-2014. Governmental Instruction for Diagnostics and Assessment of Traffic Operating Conditions of the Automobile Roads. (IIP PK 218-27-2014). Available online: https://online.zakon.kz/Document/?doc_id=37657859&pos=1;-16#pos=1;-16 (accessed on 8 November 2022).
31. ST RK 1219-2017. National Standard of the Republic of Kazakhstan for Automobile Roads and Airdromes “Methods of Measurement of Unevenness in Beddings and Covers” (CT PK 1219-2003). Available online: https://online.zakon.kz/Document/?doc_id=35447297&pos=3;-109#pos=3;-109 (accessed on 8 November 2022).
32. Badeli, S.; Carter, A.; Doré, G. Effect of laboratory compaction on the viscoelastic characteristics of an asphalt mix before and after rapid freeze-Thaw cycles. *Cold Reg. Sci. Technol.* **2018**, *146*, 98–109. [CrossRef]
33. ud Din, I.M.; Mir, M.S.; Farooq, M.A. Effect of Freeze-Thaw Cycles on the Properties of Asphalt Pavements in Cold Regions: A Review. *Transp. Res. Procedia* **2020**, *48*, 3634–3641. [CrossRef]
34. Teltayev, B.B.O.; Rossi, C.; Izmailova, G.G.; Amirbayev, E.D. Effect of Freeze-Thaw Cycles on Mechanical Characteristics of Bitumens and Stone Mastic Asphalts. *Appl. Sci.* **2019**, *9*, 458. [CrossRef]
35. Cao, H.; Chen, T.; Zhu, H.; Ren, H. Influence of Frequent Freeze-Thaw Cycles on Performance of Asphalt Pavement in High-Cold and High-Altitude Areas. *Coatings* **2022**, *12*, 752. [CrossRef]
36. Capayova, S.; Cihlarova, D.; Mondschein, P. Effect of Winter Road Maintenance on the Asphalt Road Surface—Experience in Slovakia and the Czech Republic. *Materials* **2022**, *15*, 5618. [CrossRef]
37. Cong, L.; Yang, F.; Guo, G.; Ren, M.; Shi, J.; Tan, L. The use of polyurethane for asphalt pavement engineering applications: A state-of-the-art review. *Constr. Build. Mater.* **2019**, *225*, 1012–1025. [CrossRef]
38. Guo, X.; Hao, P. Using a Random Forest Model to Predict the Location of Potential Damage on Asphalt Pavement. *Appl. Sci.* **2021**, *11*, 10396. [CrossRef]
39. Yang, S.L.; Baek, C.; Park, H.B. Effect of Aging and Moisture Damage on Fatigue Cracking Properties in Asphalt Mixtures. *Appl. Sci.* **2021**, *11*, 10543. [CrossRef]
40. Dou, J.; Yunus, A.P.; Bui, D.T.; Merghadi, A.; Sahana, M.; Zhu, Z.; Chen, C.W.; Han, Z.; Pham, B.T. Improved landslide assessment using support vector machine with bagging, boosting, and stacking ensemble machine learning framework in a mountainous watershed, Japan. *Landslides* **2020**, *17*, 641–658. [CrossRef]
41. Chen, H.-E.; Chiu, Y.-Y.; Tsai, T.-L.; Yang, J.-C. Effect of Rainfall, Runoff and Infiltration Processes on the Stability of Footholds. *Water* **2020**, *12*, 1229. [CrossRef]

42. Ivanov, V.; Arosio, D.; Tresoldi, G.; Hojat, A.; Zanzi, L.; Papini, M.; Longoni, L. Investigation on the Role of Water for the Stability of Shallow Landslides—Insights from Experimental Tests. *Water* **2020**, *12*, 1203. [[CrossRef](#)]
43. Kirschbaum, D.; Stanley, T. Satellite-based assessment of rainfall-triggered and slide hazard for situational awareness. *Earths Future* **2018**, *6*, 505–523. [[CrossRef](#)]
44. Uemoto, J.; Moriyama, T.; Nadai, A.; Kojima, S.; Umehara, T. Landslide detection based on height and amplitude differences using pre- and post-event airborne X-band SAR data. *Nat. Hazards* **2019**, *95*, 485–503. [[CrossRef](#)]
45. Zhantayev, Z.; Talgarbayeva, D.; Kairanbayeva, A.; Panyukova, D.; Turekulova, K. Complex processing of earth remote sensing data for prediction of landslide processes on roads in mountain area. *News Natl. Acad. Sci. Repub. Kazakhstan. Ser. Geol. Tech. Sci.* **2022**, *3*, 181–197. [[CrossRef](#)]